New Phytologist

Letters

Early Phosphorylated Protein 1 is required to activate the early rhizobial infection program

Introduction

Most legumes fulfill their nitrogen needs through endosymbiosis with soil diazotrophic bacteria, collectively known as rhizobia. Host legumes form specialized organs called nodules, inside which rhizobia fix atmospheric nitrogen in exchange for photo-assimilates (Lindström & Mousavi, 2020). This endosymbiosis begins with the detection by compatible rhizobia of flavonoids released by the legume host (Liu & Murray, 2016). In response, rhizobia produce and excrete lipo-chitooligosaccharides (also known as Nod Factors: NF) that are perceived on the plant side by LysM receptor-like kinases (Dénarié *et al.*, 1996; Amor *et al.*, 2003; Arrighi *et al.*, 2006; Murakami *et al.*, 2018; Rübsam *et al.*, 2023). NF perception activates the common symbiosis signaling pathway, starting with the receptor-like kinase Does not Make Infections 2 (DMI2; Stracke *et al.*, 2002), which prepares the host plant for symbiotic interactions with intracellular symbionts such as rhizobia (Radhakrishnan *et al.*, 2020; Roy *et al.*, 2020; Wang *et al.*, 2022). One of the crucial signaling events in this pathway is the rapid and sustained oscillation of the nuclear and perinuclear calcium concentration, named calcium spiking (Ehrhardt *et al.*, 1996; Kanamori *et al.*, 2006; Peiter *et al.*, 2007; Saito *et al.*, 2007; Charpentier *et al.*, 2016). The production of mevalonate via 3-hydroxy-3-methylglutaryl coenzyme a reductase 1 (HMGR1) is likely required to activate the calcium spiking (Venkateshwaran *et al.*, 2015). Decoding of these calcium signatures by the calcium- and calmodulin-dependent protein kinase CCaMK/DMI3 triggers the activation of a cohort of transcription factors, including Nodule INception (NIN), which control different stages of the root nodule symbiosis, from root-hair curling required for infection to organogenesis and the symbiont regulation (Schauser *et al.*, 1999; Marsh *et al.*, 2007; Liu *et al.*, 2019; Feng *et al.*, 2021).

Although considerable progress has been made over the past two decades in understanding the functioning of the common symbiosis signaling pathway, the mechanisms that lead to its activation still need to be better understood (Roy *et al.*, 2020). For instance, the molecular events allowing the signal transduction from the plasma membrane to the nucleus and the induction of calcium spiking remain unknown. Using phosphoproteomic analyses, we have previously identified EPP1 (Early Phosphorylated Protein 1) in *Medicago truncatula* to be phosphorylated at Serine 77 (S77) 1 h after treatment with purified NF (Rose *et al.*, 2012). Further transcriptional characterization demonstrated that the expression of *MtEPP1* is dependent on NF perception (Valdés-López *et al.*, 2019). Downregulation of *MtEPP1* by RNA interference (RNAi) showed that MtEPP1 is required for NF-triggered calcium spiking (Valdés-López *et al.*, 2019). Furthermore, the number of nodules decreased by 90% in the *MtEPP1*-RNAi transgenic roots compared with control roots (Valdés-López *et al.*, 2019). This *MtEPP1* knock-down phenotype led us to hypothesize that MtEPP1 may contribute to the common symbiosis signaling pathway immediately after perceiving NF at the plasma membrane. Here, we further investigated the role of MtEPP1 in the common symbiotic signaling pathway.

Materials and Methods

Plant material and growth conditions

Medicago truncatula line Jemalong A17, *dmi2*-TR25, *dmi1*-B129, and *dmi3*-TRV25 mutants derived from Jemalong (Ané *et al.*, 2002) were used in this study. Six stable *MtEPP1*-RNAi transgenic lines (L1a, L28a, L28b, L31, L38, and L43) were generated in the genetic background R108. The *MtEPP1*-RNAi lines were generated using the pK7FWG2-RR vector expressing the dsRed reporter gene. The kanamycin-resistant plants were screened for red fluorescence under the fluorescent stereo zoom microscope. Only plants expressing dsRed were used for root nodulation or expression profiling assays. Seed germination was performed as previously described (Valdés-López *et al.*, 2019). All plants were grown in a growth chamber at 22°C with a 16 h : 8 h, light : dark photoperiod.

Bacterial strains and culture conditions

The empty vector pBA-DC-TDT was amplified in *Escherichia coli* DB3.1 cells. By contrast, the *MtEPP1* overexpression constructs (see below for details) were amplified in *E. coli* DH5α cells. *Escherichia coli* cells were handled using standard protocols.

Agrobacterium rhizogenes MSU440 strain was used to induce transgenic roots in *M. truncatula* plants (see below for details). *Agrobacterium rhizogenes* cells were grown on 5 mg l^{-1} tryptone/3 mg l^{-1} yeast extract, 6 mM $CaCl_2$ (TY) plates for 2 d at 30°C in the presence of 50 μg ml^{-1} spectinomycin or 50 μg ml^{-1} kanamycin to select for the presence of vectors.

Sinorhizobium meliloti was used to inoculate *M. truncatula* plants for nodulation assays. *Sinorhizobium meliloti* cells were grown on TY plates supplemented with 50 μg ml^{-1} streptomycin for 2 d at 30°C.

Plasmid construction

To generate the *MtEPP1* wild-type (WT) overexpression construct, the full CDS (coding sequence) of *MtEPP1* was amplified from *M. truncatula* root cDNA using primers 5′-caccatgggaacaaatag ccaggagcat-3′ and 5′-tcattcaactacctgagatgaagcagc-3′. The PCR product was then cloned into pENTR-D-TOPO vector (Thermo Fisher Scientific, Waltham, MA, USA). The resulting pENTR-*MtEPP1* plasmid was recombined into the pBA-DC-TDT binary vector yielding the pBA-*MtEPP1*$_{(Wt)}$-TDT construct (hereafter referred to as *MtEPP1*$_{(Wt)}$-Ox).

For overexpression of the phosphomimetic MtEPP1 version, the sequence was mutated on serine S77 using primers 5′-gatattagatggg atggtccaatca-3′ and 5′-tgattggaccatcccatctaatatc-3′. The PCR product was then cloned into pENTR-D-TOPO vector (Thermo Fisher Scientific). The resulting pENTR-*MtEPP1*$_{(S-D)}$ plasmid was recombined into the pBA-DC-TDT binary vector yielding the pBA-*MtEPP1*$_{(S-D)}$-TDT construct (hereafter referred to as *MtEPP1*$_{(S-D)}$-Ox).

Agrobacterium rhizogenes-mediated transformation

Binary vectors with *MtEPP1*$_{(Wt)}$-Ox or *MtEPP1*$_{(S-D)}$-Ox constructs were mobilized into *A. rhizogenes* MSU440 by electroporation. The empty vector pBA-DC-TDT was used as a control. *Agrobacterium rhizogenes*-mediated transformation was performed according to Boisson-Dernier *et al.* (2001). Composite plants (plants with the transformed root system and untransformed shoot system) were grown in nitrogen-free Fahräeus medium plates under the environmental conditions described previously. TDT fluorescence in the transgenic roots was observed with a fluorescence stereomicroscope.

Gene expression analysis

To analyze the expression of *MtNIN*, *MtNF-YB*, and *MtERN1*, composite plants with transgenic roots expressing either an empty vector (control), *MtEPP1*$_{(Wt)}$-Ox or *MtEPP1*$_{(S-D)}$-Ox constructs were grown in Fahräeus medium plates for 3 wk under sterile conditions. Stable *MtEPP1*-RNAi lines and R108 control were grown in growth pouches for a week under sterile conditions. Six stable RNAi lines showing a significant decrease in nodule numbers were analyzed for RT-qPCR-based expression profiling. Transgenic roots showing TDT or dsRed fluorescence were harvested, immediately frozen in liquid nitrogen, and stored at −80°C. Total RNA was isolated from transgenic roots from 10 different composite plants using the ZR Plant RNA miniprep kit (Zymo Research, Irvine, CA, USA) following the manufacturer's instructions. cDNAs were synthesized from 1 μg of genomic DNA-free total RNAs and used to analyze gene expression by RT-qPCR, as we previously described in Valdés-López *et al.* (2019). RT-qPCR primer sequences used in this study were previously reported by Valdés-López *et al.* (2019). Five biological replicates, each one with five technical replicates, were included in this experiment.

Preparation of messenger RNA-Seq libraries and next-generation sequencing

Total RNA was isolated from 0.5 g of *M. truncatula* Jemalong A17 transgenic roots expressing an empty vector (Control), *MtEPP1*$_{(Wt)}$-Ox or *MtEPP1*$_{(S-D)}$-Ox constructs and growing under sterile conditions. Stranded messenger RNA-seq (mRNA-seq) libraries were generated from 1 μg of genomic DNA-free total RNA from each experimental condition and prepared using the TruSeq RNA Sample Prep kit (Illumina, San Diego, CA, USA) according to the manufacturer's instructions. Three biological replicates containing transgenic roots from 20 independent composite plants were included for each experimental condition. Nine libraries were sequenced on an Illumina NextSeq 500 platform with a 150-cycle sequencing kit and a configuration of paired-end reads with a 75-bp read length. Library construction and sequencing were performed by the Unidad Universitaria de Secuenciación Masiva y Bioinformática (Instituto de Biotecnología, UNAM, México).

Mapping and processing messenger RNA-Seq reads

Adapter and contamination removal were carried out using in-house Perl scripts. Sequences were filtered based on quality (Q33, FASTQ Quality Filter v.0.0.13, http://hannonlab.cshl.edu/fastx_toolkit/index.html). About 20 million reads per sample were aligned to the *M. truncatula* transcriptome (V5 from INRA MtrunA17r5.0-ANR) using BOWTIE2 (v.2.3.5) using the recommended parameters to match RSEM analysis input requirements (Langmead & Salzberg, 2012). Gene expression was calculated using the RNA-seq by Expectation Maximization (RSEM) method (v.1.3.3) and the default parameters (Li & Dewey, 2011). Significantly differentially expressed genes (DEGs: adjusted *P*-value ≤ 0.01) were identified using DESEQ2, part of the Integrated Differential Expression Analysis MultiEXperiment (IDEAMEX) platform (Jiménez-Jacinto *et al.*, 2019), with the RSEM expected counts. Gene Ontology (GO) term enrichment analyses were performed using AGRIGO (v.2.0) and default parameters (FDR cutoff = 0.05; Tian *et al.*, 2017).

Root-hair deformation analysis

Medicago truncatula Jemalong A17 and *dmi2* composite plants expressing an empty vector, *MtEPP1*$_{(Wt)}$-OX or *MtEPP1*$_{(S-D)}$-OX constructs and growing in Fahräeus plates were treated with 10 nM purified NFs from *S. meliloti*. Upon 16 h of treatment, transgenic roots showing TDT fluorescence were observed with a bright-field microscope. Twenty biological replicates, each one with 10 plants, were included in this experiment.

Nodulation assays

Medicago truncatula Jemalong A17 composite plants expressing an empty vector or the *MtEPP1*$_{(Wt)}$-OX or *MtEPP1*$_{(S-D)}$-OX constructs and growing in pots filled with wet perlite were inoculated with 1 ml of *S. meliloti* solution (OD_{600}: 0.03). At 30 d

New Phytologist

postinoculation, the total number of nodules was counted in roots showing red fluorescence exclusively. For this experiment, 10 biological replicates, each one containing 20 plants, were used.

Medicago truncatula MtEPP1-RNAi stable transgenic and WT R108 plants were grown in growth pouches supplemented with modified Fähraeus media. After 7 d of growth, plants were inoculated with *S. meliloti* (OD_{600}: 0.05). At 14 d postinoculation, the total number of nodules was counted. Three biological replicates, each containing 10 plants, were used for this experiment, and the nodule numbers were counted only from plants showing bright red fluorescence. One-way ANOVA followed by a Tukey honest significant difference (HSD) test was performed to test the statistical significance of the data.

Results and Discussion

NF-triggered root-hair branching, calcium spiking, and nodule development are significantly reduced in *M. truncatula MtEPP1*-RNAi roots (Valdés-López *et al.*, 2019). Indeed, nodulation assays in stable *MtEPP1*-RNAi transgenic lines confirmed that the downregulation of *MtEPP1* significantly reduces the formation of nodules in *M. truncatula* (Supporting Information Fig. S1a). All six EPP1 RNAi lines showed a decrease in nodule number compared with the WT parent R108. However, L28a and L31 showed a significant decrease of *c.* 85% nodule numbers compared with the control. Similarly, the expression of *MtEPP1* in these two lines was significantly reduced compared with R108 and other RNAi lines (Fig. S1b). Overexpression of gain-of-function versions of genes acting in the common symbiosis pathway leads to increased activation of symbiotic responses such as gene induction and root-hair deformation (Gleason *et al.*, 2006; Tirichine *et al.*, 2006; Singh *et al.*, 2014). To further test that MtEPP1 could participate in the common symbiosis signaling pathway, we evaluated the effect of overexpressing the WT version of *MtEPP1* in the Jemalong A17 WT background. We observed no significant differences in the number of NF-triggered root-hair branching in $MtEPP1_{(Wt)}$-Ox transgenic roots compared with control roots (Fig. S2a). Because MtEPP1 is highly phosphorylated at S77 in response to NF (Valdés-López *et al.*, 2019), we generated a phosphomimetic version of MtEPP1 by substituting S77 with a negatively charged Aspartic Acid residue ($MtEPP1_{(S\text{-}D)}$). Overexpression of $MtEPP1_{(S\text{-}D)}$ in transgenic roots resulted in a 50% increase in NF-triggered roots hair branching compared with control or $MtEPP1_{(Wt)}$-Ox transgenic roots (Fig. S2a). Next, we evaluated whether the overexpression of *MtEPP1* influences nodule formation. We observed that $MtEPP1_{(Wt)}$-Ox roots developed the same number of nodules than control roots, whereas $MtEPP1_{(S\text{-}D)}$-Ox roots developed 40% more nodules compared with control and $MtEPP1_{(Wt)}$-Ox roots (Fig. S2b).

Swollen root hairs are a characteristic phenotype in *dmi2* mutant plants in response to rhizobia or purified NF (Catoira *et al.*, 2000). This phenotype indicates that early signal transduction after bacteria perception and infection is compromised in *dmi2* mutants (Catoira *et al.*, 2000). The fact that $MtEPP1_{(S\text{-}D)}$-Ox transgenic roots developed a higher number of branched root hairs in response to purified NF (Fig. S2a) prompted us to evaluate whether the overexpression of $MtEPP1_{(S\text{-}D)}$ in *dmi2* mutants could reestablish a WT-like root-hair branching phenotype in response to purified NF. As anticipated, *dmi2* transgenic roots transformed with an empty vector or overexpressing $MtEPP1_{(Wt)}$ developed a majority of swollen root hairs (Fig. S2c). By contrast, *dmi2* transgenic roots overexpressing $MtEPP1_{(S\text{-}D)}$ developed more branched root hairs than swollen ones (Fig. S2c). These phenotypic data support a model where MtEPP1 phosphorylation upon NF perception is required to decode the NF signal and activate the early rhizobial infection program.

Overexpression of $MtEPP1_{(S\text{-}D)}$ increases the number of NF-triggered root-hair branching and number of nodules in WT *M. truncatula* plants and partially restores root-hair branching phenotype in *dmi2* mutant plants. Autoactivation of the common symbiosis signaling pathway is known to induce the expression of symbiotic marker genes (Gleason *et al.*, 2006; Tirichine *et al.*, 2006; Singh *et al.*, 2014). We therefore tested the ability of $MtEPP1_{(Wt)}$-Ox or $MtEPP1_{(S\text{-}D)}$-Ox to induce *MtERN1*, *MtNF-YB*, and *MtNIN*, which are all required to activate the early rhizobial infection and nodule development programs (Schauser *et al.*, 1999; Boisson-Dernier *et al.*, 2005; Wan *et al.*, 2007; Cerri *et al.*, 2012). First, we assessed the expression of these symbiotic genes in Jemalong A17 transgenic roots expressing an empty vector (control), $MtEPP1_{(Wt)}$-Ox or $MtEPP1_{(S\text{-}D)}$-Ox and in the absence of rhizobia or purified NF. This expression analysis revealed that the overexpression of $MtEPP1_{(Wt)}$ was twice higher than in $MtEPP1_{(S\text{-}D)}$ (Fig. 1a). Furthermore, in the absence of rhizobia or purified NF, the overexpression of *MtEPP1*, regardless of the version (Wt or S77D), significantly increased the expression of *MtERN1*, *MtNF-YB*, and *MtNIN* (Fig. 1a). However, despite the lower overexpression levels of $MtEPP1_{(S\text{-}D)}$, the expression of these symbiotic genes was significantly higher. Indeed, *MtNIN* was twice expressed in $MtEPP1_{(S\text{-}D)}$ than in $MtEPP1_{(Wt)}$ roots (Fig. 1a). These expression profiles mirror the significant reduction in the expression of these symbiotic genes in response to purified NFs when knocking down *MtEPP1* (Valdés-López *et al.*, 2019).

We performed a similar expression analysis in the *dmi1*, *dmi2*, and *dmi3* backgrounds. We observed that regardless of the version of *MtEPP1* used, its overexpression increased the expression of *MtERN1*, *MtNF-YB*, and *MtNIN* in the absence of rhizobia or purified NF in the *dmi2* background but not in the *dmi1* and *dmi3* mutants (Fig. 1b–d). Interestingly, we also observed that the lower overexpression levels of $MtEPP1_{(S\text{-}D)}$ have a more substantial effect on the expression of these symbiotic genes, particularly *MtNIN*, than in $MtEPP1_{(Wt)}$ roots (Fig. 1b).

To get further insights into the symbiotic genes that MtEPP1 might regulate, we performed an RNA-seq analysis in Jemalong A17 transgenic roots expressing an empty vector, $MtEPP1_{(Wt)}$-Ox or $MtEPP1_{(S\text{-}D)}$-Ox, and in the absence of rhizobia and purified NF. Principal component analysis showed a clustering of biological replicates and overexpressing-depending variation, with the first component explaining an average of 57% of data variation (Fig. S3). Gene Ontology (GO) enrichment analysis revealed that GO terms related to cell wall remodeling were the most significantly enriched in the upregulated genes from $MtEPP1_{(Wt)}$-Ox and $MtEPP1_{(S\text{-}D)}$-Ox roots (Fig. S4).

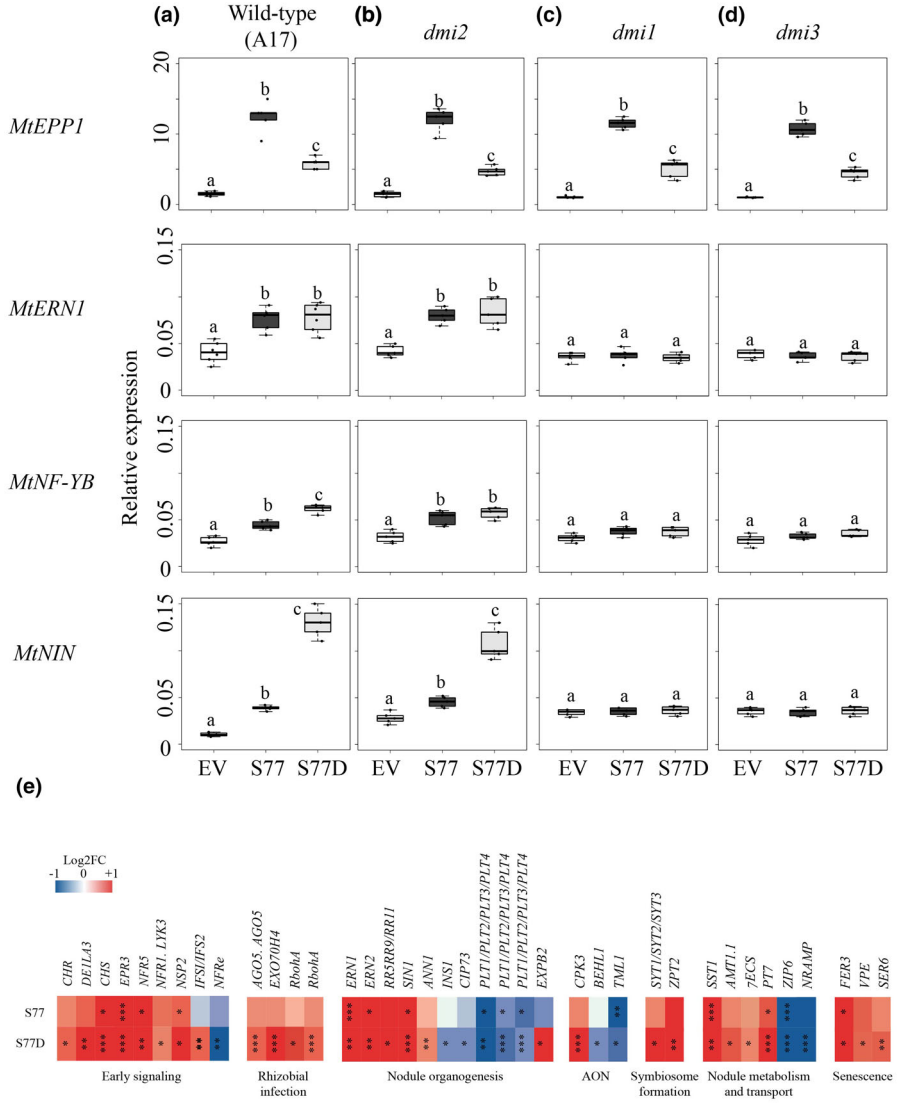

Fig. 1 Overexpression of *MtEPP1* is sufficient to activate the expression of symbiotic genes in *Medicago truncatula*. Expression levels of *MtEearly Phosphorylated Protein1* (*MtEPP1*), *MtERF Required for Nodulation1* (*MtERN1*), *MtNuclear Factor-YB* (*MtNF-YB*), and *MtNodule Inception* (*MtNIN*) in transgenic roots generated in the wild-type (WT; Jemalong A17) (a), *dmi2* (b), *dmi1* (c), and *dmi3* (d) genetic backgrounds expressing an empty vector (EV) or the $MtEPP1_{(Wt)}$-OX (S77) or $MtEPP1_{(S\text{-}D)}$-OX (S77D) constructs. Box plots represent the first and third quartile (horizontal box sides) and the minimum and maximum (outside whiskers). Data were obtained from five biological replicates, each with five technical replicates. One-way ANOVA followed by a Tukey honest significant difference (HSD) test was performed (*P*-value < 0.01). Statistical classes sharing a letter are not significantly different. (e) Heatmap showing $\log_2$ fold-change of gene transcripts involved in early signaling, rhizobial infection, nodule organogenesis, autoregulation of nodulation (AON), symbiosome formation, nodule metabolism and transport, and senescence. Genes showing higher and lower expression differences are shown in shades of red and blue, respectively. S77: differentially regulated genes in the comparison between $MtEPP1_{(Wt)}$-Ox and empty vector roots; S77D: differentially regulated genes in the comparison between $MtEPP1_{(S\text{-}D)}$-Ox and empty vector roots. Asterisks indicate different levels of statistical significance of the comparisons (*, adjusted *P*-values < 0.05; **, adjusted *P*-value < 0.01; ***, adjusted *P*-value < 0.001). Genes with no asterisk are not significantly differentially expressed.

Furthermore, our RNA-seq analysis revealed that $MtEPP1_{(S\text{-}D)}$-Ox transgenic roots displayed numerous upregulated genes participating in early signaling (i.e. *DELLA3*, *NSP2*, and *ISF1/2*), rhizobial infection (i.e. *ERN1*, *ERN2*, *EXO70H4*, and *RbohA*), and nodule organogenesis (i.e. *SIN1*) compared with control transgenic roots (Fig. 1e). A few genes participating in these stages of the root nodule symbiosis were also upregulated in $MtEPP1_{(Wt)}$-Ox roots (Fig. 1e). Interestingly, we observed that the expression of genes conforming the autoregulation of nodulation pathway (AON), which negatively regulates the formation of nodules (Ferguson *et al.*, 2019), was significantly downregulated in $MtEPP1_{(S\text{-}D)}$-Ox roots (Figs 1e, S5). This expression pattern of AON-related genes is in line with the increase in the number of nodules observed in $MtEPP1_{(S\text{-}D)}$-Ox roots.

Comparing our RNA-seq profiles with a previous study of NF-regulated genes (Damiani *et al.*, 2016) revealed an overlap of 9% and 25% between the differentially regulated genes by NF in A17 Jemalong WT roots and $MtEPP1_{(Wt)}$-Ox or $MtEPP1_{(S\text{-}D)}$-Ox roots, respectively (Fig. S6a). We also observed that genes with known roles in NF signaling, rhizobial infection, nodule organogenesis, AON, and nitrogen fixation were significantly induced by $MtEPP1_{(S\text{-}D)}$ in the absence of purified NF or rhizobia (Fig. S6b). Altogether, these transcriptional analyses confirm that MtEPP1 is sufficient to activate the common symbiotic signaling pathway, particularly in activating the early rhizobial infection program.

Given the fact that the overexpression of *MtEPP1* is required to activate the expression of symbiotic genes that are essential to activate the rhizobial infection and some for nodule development, we investigated whether the overexpression of *MtEPP1* can lead to the formation of spontaneous nodules. However, despite many attempts, we observed no spontaneous nodules regardless of the version of *MtEPP1* used (Table S1).

These data indicate that MtEPP1 activation downstream of DMI2 is required for symbiotic signaling. The partial complementation of the *dmi2* phenotype and the induction of gene expression in the WT and *dmi2* background but not in the *dmi1* and *dmi3* background position MtEPP1 as one of the missing links between the plasma membrane and the events occurring in the nucleus in the common symbiosis signaling pathway (Fig. 2). Further investigation is needed to understand the mechanism of action of MtEPP1 in the activation of the common symbiotic signaling pathway.

New Phytologist

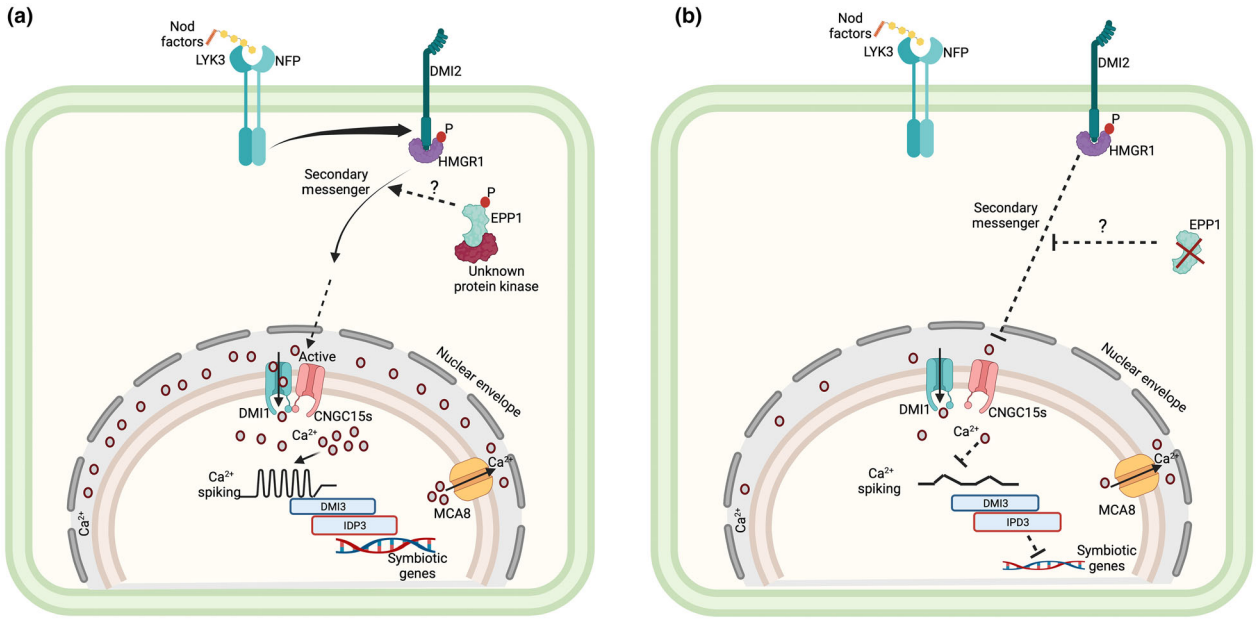

Fig. 2 Proposed model for MtEPP1 in activating the common symbiotic signaling pathway. (a) Nod Factors are perceived by Nod Factor Perception (NFP) and Lysin Motif Receptor-Like Kinase3 (LYK3) plasma membrane receptors. Subsequently, the co-receptor Does not Make Infections2 (DMI2) is activated and interacts with 3-hydroxy-3-methylglutaryl coenzyme a reductase 1 (HMGR1) leading to the production of mevalonate, which likely acts as a second messenger. Based on our data, we proposed that, upon phosphorylation by a yet-unknown protein kinase, MtEPP1 acts downstream of DMI2. The active form of MtEPP1 might contribute to the production of secondary messengers required to promote the interaction between DMI1 and the cyclic nucleotide-gated channel 15 (CNGC15s). This protein–protein interaction is needed to activate the calcium (Ca^{2+}) spiking decoded by the Does not Make Infections3 (DMI3)-Interacting Protein of DMI3IPD3 complex. (b) Without the active form of MtEPP1, the production of second messengers might be compromised, and the subsequent activation of Does not Make Infections (1) (DMI1) and the calcium spiking is inhibited. The absence of this calcium signature inhibits the expression of crucial genes required to establish symbiosis with rhizobia. Dashed arrows depict a potential positive role, whereas blunt-ended dashed lines represents inhibitory effect. Images were created with BioRender (https://biorender.com).

Acknowledgements

This work was supported by the Programa de Apoyo a Proyectos de Investigación e Innovación Tecnológica (PAPIIT grant No. IN201320) to OV-L MCI-A is a Royal Society Newton International Fellow. Research performed at LRSV was also supported by the 'Laboratoires d'Excellence (LABEX)' TULIP (ANR-10-LABX-41), by the project Engineering Nitrogen Symbiosis for Africa (ENSA) funded through a grant to the University of Cambridge by the Bill and Melinda Gates Foundation (OPP1172165) and the UK Foreign, Commonwealth and Development Office as Engineering Nitrogen Symbiosis for Africa (OPP1172165). This project received funding from the European Research Council (ERC) under the European Union's Horizon 2020 research and innovation program (grant agreement no. 101001675 – ORIGINS) to P-MD. JMA acknowledges support from the National Science Foundation – Integrative Organismal Systems (NSF-IOS: 2010789) and the Department of Energy (DOE: DE-SC0018247). We thank Georgina Hernández (Centro de Ciencias Genómicas, UNAM. México) and Kiwamu Tanaka (Washington State University, USA) for constructive discussion. We are grateful to María del Socorro Sánchez-Correa (FES Iztacala, UNAM. México) and María Montserrat González-Hernández for technical assistance and create a high-resolution version of Fig. 1, respectively.

Competing interests

None declared.

Author contributions

OV-L, P-MD and J-MA designed the work and drafted the manuscript; SF-O, MCI-A, EAP-R, MT, TV, MKR and MM performed the experiments. DF, SF-O and OV-L analyzed the data. All authors contributed to the final version of the manuscript.

ORCID

Jean-Michel Ané https://orcid.org/0000-0002-3128-9439
Pierre-Marc Delaux https://orcid.org/0000-0002-6211-157X
Susana Ferrer-Orgaz https://orcid.org/0009-0002-6207-2854
Damien Formey https://orcid.org/0000-0003-2852-4706
Mariel C. Isidra-Arellano https://orcid.org/0000-0002-7121-4589
Malick Mbengue https://orcid.org/0000-0002-7723-7757
Eithan A. Pozas-Rodriguez https://orcid.org/0009-0000-2133-872X
Manish Tiwari https://orcid.org/0000-0002-3994-6181
Oswaldo Valdés-López https://orcid.org/0000-0002-4760-048X

Data availability

The original contributions presented in the study are publicly available. The RNA-seq data presented in this study are deposited in the BioProject repository, accession no. PRJNA994923 (https://www.ncbi.nlm.nih.gov/bioproject/PRJNA994923).

Susana Ferrer-Orgaz[1,2], Manish Tiwari[3], Mariel C. Isidra-Arellano[1,4], Eithan A. Pozas-Rodriguez[1,2], Tatiana Vernié[5], Mélanie K. Rich[5], Malick Mbengue[5], Damien Formey[6], Pierre-Marc Delaux[5], Jean-Michel Ané[3,7] and Oswaldo Valdés-López[1]*

[1]Laboratorio de Genómica Funcional de Leguminosas, Facultad de Estudios Superiores Iztacala, Universidad Nacional Autónoma de México, Tlalnepantla, 54090, Mexico; [2]Department of Plant Pathology, Russell Laboratories, University of Wisconsin, 1630 Linden Dr., Madison, WI 53706, USA; [3]Department of Bacteriology, University of Wisconsin, Microbial Science Building, 1550 Linden Dr., Madison, WI 53706, USA; [4]Royal Botanic Gardens, Kew, Richmond, Surrey, TW9 3AE, UK; [5]Laboratoire de Recherche en Sciences Végétales (LRSV), Université de Toulouse, CNRS, UPS, 24 chemin de Borde Rouge, Auzeville, BP42617, 3126, Castanet Tolosan, France; [6]Centro de Ciencias Genómicas, Universidad Nacional Autónoma de México, Cuernavaca, 62210, Morelos, Mexico; [7]Department of Agronomy, University of Wisconsin, 1575 Linden Dr., Madison, WI 53706, USA

(*Author for correspondence: email oswaldovaldesl@unam.mx)

References

Amor BB, Shaw SL, Oldroyd GE, Maillet F, Menmetsa RV, Cook D. 2003. The NFP locus of *Medicago truncatula* controls an early step of Nof factor signal transduction upstream of a rapid calcium flux and root hair deformation. *The Plant Journal* **34**: 495–506.

Ané JM, Lévy J, Thoquet P, Kulikova O, de Billy F, Penmetsa V, Kim DK, Debellé F, Rosenberg C, Cook DR *et al.* 2002. Genetic and cytogenetic mapping of DMI1, DMI2, and DMI3 genes of *Medicago truncatula* involved in Nod factor transduction, nodulation, and mycorrhization. *Molecular Plant–Microbe Interactions* **15**: 1108–1118.

Arrighi JF, Barre A, Ben Amor B, Bersoult A, Campos Soriana L, Mirabella R, de Carvalho-Niebel F, Journet EP, Ghérardi M, Huguet T *et al.* 2006. The *Medicago truncatula* lysin motif-receptor-like kinase gene family includes *NFP* and new nodule-expressed genes. *Plant Physiology* **142**: 265–279.

Boisson-Dernier A, Andriankaja A, Chabaud M, Niebel A, Journet EP, Barker DG, de Carvalho-Niebel F. 2005. *MtENOD11* gene activation during rhizobial infection and mycorrhizal arbuscule development requires a common AT-rich-containing regulatory sequence. *Molecular Plant–Microbe Interactions* **18**: 1269–1276.

Boisson-Dernier A, Chabaud M, Garcia F, Bécard G, Rosenberg C, Barker DC. 2001. *Agrobacterium rhizogenes*-transformed roots of *Medicago truncatula* for the study of nitrogen-fixing and endomycorrhizal symbiotic associations. *Molecular Plant–Microbe Interactions* **14**: 695–700.

Catoira R, Galera C, de Billy F, Penmetsa RV, Journet EP, Maillet F, Rosenberg C, Cook D, Gough C, Dénarié J. 2000. Four genes of *Medicago truncatula* controlling components of a Nod factor transduction pathway. *Plant Cell* **12**: 1647–1665.

Cerri MR, Frances L, Laloum T, Auria MC, Niebel A, Oldroyd GED, Barker DG, Fournier J, de Carvalho-Niebel F. 2012. *Medicago trucatula* ERN transcription factors: regulatory interplay with NSP1/NSP2 GRAS factors and expression dynamics throughout rhizobial infection. *Plant Physiology* **160**: 2155–2172.

Charpentier M, Sun J, Vas Martins T, Radhakrishnan GV, Findlay K, Soumpourou E, Thouin J, Véry AA, Sanders D, Morris R *et al.* 2016. Nuclear-localized cyclic nucleotide-gated channels mediate symbiotic calcium oscillations. *Science* **352**: 1102–1105.

Damiani I, Drain A, Guichard M, Balzergue S, Boascari A, Boyer JC, Brunaud V, Cottaz S, Rancurel C, Da Rocha M *et al.* 2016. Nod Factors effects on root hair-specific transcriptome of *Medicago truncatula*: plasma membrane transport systems and reactive oxygen species networks. *Frontiers in Plant Science* **7**: 794.

Dénarié J, Debellé F, Promé JC. 1996. Rhizobium lipo-chitooligosaccharide nodulation factor: signaling molecules mediating recognition and morphogenesis. *Annual Review of Biochemistry* **65**: 503–535.

Ehrhardt DW, Wais R, Long SR. 1996. Calcium spiking in plant root hairs responding to rhizobium nodulation signals. *Cell* **85**: 673–681.

Feng J, Lee T, Schiessl K, Oldroyd GED. 2021. Processing of NODULE INCEPTION controls the transition to nitrogen fixation in root nodules. *Science* **374**: 629–632.

Ferguson BJ, Mens C, Hastwell AH, Zhang M, Su H, Jones CH, Chu X, Gresshoff PM. 2019. Legume nodulation: the host controls the party. *Plant, Cell & Environment* **42**: 41–51.

Gleason G, Chaudhuri S, Yang T, Muñoz A, Poovaiah BW, Oldroyd GED. 2006. Nodulation independent of rhizobia induced by a calcium-activated kinase lacking autoinhibition. *Nature* **44**: 1149–1152.

Jiménez-Jacinto V, Sanchez-Flores A, Vega-Alvarado L. 2019. Integrative Differential Expression Analysis for Multiple EXpreriments (IDEAMEX): a web server tool for integrated RNA-Seq data analysis. *Frontiers in Genetics* **10**: 279.

Kanamori N, Madsen LH, Radutoiu S, Frantescu M, Quistgaard EMH, Miwa H, Downie JA, James EK, Felle HH, Lindegaard L *et al.* 2006. A nucleoporin is required for induction of Ca^{2+} spiking in legume nodule development and essential for rhizobial and fungal symbiosis. *Proceedings of the National Academy of Sciences, USA* **103**: 359–364.

Langmead B, Salzberg SL. 2012. Fast gapped-read alignment with BOWTIE 2. *Nature Methods* **9**: 357–359.

Li H, Dewey CN. 2011. RSEM: accurate transcript quantification from RNA-seq data with or without a reference genome. *BMC Bioinformatics* **12**: 323.

Lindström K, Mousavi A. 2020. Effectiveness of nitrogen fixation in rhizobia. *Microbial Biotechnology* **13**: 1314–1335.

Liu CW, Breakspear A, Guan D, Cerri MR, Jackson K, Jiang SY, Robson F, Radhakrishnan GV, Roy S, Bone C *et al.* 2019. NIN acts as a network hub controlling a growth module required for rhizobial infection. *Plant Physiology* **179**: 1704–1722.

Liu CW, Murray JD. 2016. The role of flavonoids in nodulation host-range specificity: an update. *Plants* **5**: 33.

Marsh JF, Rakocevic A, Mitra RM, Brocard L, Sun J, Eschtruth A, Long SR, Schultze M, Ratet P, Oldroyd GE. 2007. *Medicago truncatula* NIN is essential for rhizobial-independent nodule organogenesis induced by autoactive calcium/calmodulin-dependent protein kinase. *Plant Physiology* **144**: 324–335.

Murakami E, Cheng J, Gysel K, Bozsoki Z, Kawaharada Y, Hjuler CT, Sorensen KK, Tao K, Kelly S, Venice F. 2018. Epidermal LysM receptor ensures robust symbiotic signaling in *Lotus japonicus*. *eLife* **7**: e33506.

Peiter E, Sun J, Heckmann AB, Venkateshwaran M, Riely BK, Otegui MS, Edwards A, Freshour G, Hahn MG, Cook DR *et al.* 2007. The *Medicago truncatula* DMI1 protein modulates cytosolic calcium signaling. *Plant Physiology* **145**: 192–203.

Radhakrishnan G, Keller J, Rich MK, Vernié T, Mbadinga Mbadinga DL, Vigneron N, Cottret L, San Clemente H, Libourel C, Cheema J *et al.* 2020. An ancestral signaling pathway is conserved in intracellular symbioses-forming plant lineages. *Nature Plants* **6**: 280–289.

Rose CM, Venkateshwaran M, Vokening JD, Grimsrud PA, Maeda J, Bailey DJ, Park K, Howes-Podoll M, den Os D, Yeun LH *et al.* 2012. Rapid phosphoproteomic and transcriptomic changes in the rhizobia-legume symbiosis. *Molecular Cell Proteomics* **11**: 724–744.

Roy S, Liu W, Nandety RS, Crook A, Mysore KS, Pislariu CI, Frugoli J, Dicstein R, Udvardi MK. 2020. Celebrating 20 years of genetic discoveries in legume nodulation and symbiotic nitrogen fixation. *Plant Cell* **32**: 15–41.

Rübsam H, Krönauer C, Abel NJB, Ji H, Lironi D, Hansen SB, Nadzieja M, Kolte MV, Abel D, Jong ND. 2023. Nanobody-driven signaling reveals the core receptor complex in root nodule symbiosis. *Science* **379**: 272–277.

Saito K, Yoshikawa M, Yano K, Miwa H, Uchida H, Asamizu E, Sato S, Tabata S, Imaizumi-Anraku H, Umehara Y *et al.* 2007. NUCLEOPORIN85 is required

for calcium spiking, fungal and bacterial symbiosis, and seed production in *Lotus japonicus*. *Plant Cell* **19**: 610–624.

Schauser L, Roussis A, Stiller J, Stougaard J. 1999. A plant regulator controlling development of symbiotic root nodules. *Nature* **402**: 191–195.

Singh S, Katzer K, Lambert J, Cerri M, Parniske M. 2014. CYCLOPS, a DNA-binding transcriptional activator, orchestrates symbiotic root nodule development. *Cell Host & Microbe* **15**: 139–152.

Stracke S, Kistner C, Yoshida S, Mulder L, Sato S, Kaneko T, Tabata S, Sandal N, Stougaard J, Szczyglowski K *et al.* 2002. A plant receptor-like kinase required for both bacterial and fungal symbiosis. *Nature* **417**: 959–962.

Tian T, Liu Y, Yan H, You Q, Yi X, Du Z, Xu W, Su Z. 2017. AGRIGO v.2.0: a GO analysis toolkit for the agricultural community, 2017 update. *Nucleic Acids Research* **45**: W122–W129.

Tirichine L, Imaizumi-Anraku H, Yoshida S, Murakami Y, Madsen LH, Miwa H, Nakagawa T, Sandal N, Albrektsen AS, Kawaguchi M *et al.* 2006. Deregulation of a Ca^{2+}/calmodulin-dependent kinase leads to spontaneous nodule development. *Nature* **44**: 1153–1156.

Valdés-López O, Jayaraman D, Maeda J, Delaux PM, Venkateshwaran M, Isidra-Arellano MC, Reyero-Saavedra MDR, Sánchez-Correa MDS, Verastegui-Vidal MA, Delgado-Buenrostro N *et al.* 2019. A novel positive regulator of the early stages of root nodule symbiosis identified by phosphoproteomics. *Plant & Cell Physiology* **60**: 575–586.

Venkateshwaran M, Jayaraman D, Chabaud M, Genre A, Ballon AJ, Maeda J, Forshey K, den Os D, Kwiecien NW, Coon JJ *et al.* 2015. A role for the mevalonate pathway in early plant symbiotic signaling. *Proceedings of the National Academy of Sciences, USA* **112**: 9781–9786.

Wan X, Hontelez J, Lillo A, Guarneiro C, van de Peut D, Federova E, Bisseling T, Franssen H. 2007. *Medicago truncatula ENOD40-1* and *ENOD40-2* are both involved in nodule initiation and bacteroid development. *Journal of Experimental Botany* **58**: 2033–2041.

Wang D, Dong W, Murray J, Wang E. 2022. Innovation and appropriation in mycorrhizal and rhizobial symbioses. *Plant Cell* **34**: 1573–1599.

Supporting Information

Additional Supporting Information may be found online in the Supporting Information section at the end of the article.

Fig. S1 Downregulation of *MtEPP1* significantly reduces nodule formation in stable transgenic *Medicago truncatula* plants.

Fig. S2 Overexpression of $MtEPP1_{(S\text{-}D)}$ increases the number of Nod Factor-triggered deformed root hair and partially reestablishes this phenotype in the *dmi2* mutant background.

Fig. S3 Principal component analysis of the RNA-seq dataset.

Fig. S4 Gene ontology terms significantly enriched in the differentially expressed genes in *Medicago truncatula* transgenic roots expressing the $MtEPP1_{(Wt)}$-OX or $MtEPP1_{(S\text{-}D)}$-OX constructs.

Fig. S5 Overexpression of *MtEPP1* downregulates the expression of autoregulation of nodulation-related genes.

Fig. S6 Overexpression of *MtEPP1* constitutively activates symbiotic genes required for signaling, rhizobial infection, and nodule development.

Table S1 Overexpression of *MtEPP1* does not confer spontaneous nodulation in *Medicago truncatula*.

Please note: Wiley is not responsible for the content or functionality of any Supporting Information supplied by the authors. Any queries (other than missing material) should be directed to the *New Phytologist* Central Office.

Key words: common symbiosis signaling pathway, *Medicago truncatula*, *MtDMI1*, *MtDMI2*, *MtDMI3*, root nodule symbiosis.

Received, 7 August 2023; accepted, 9 November 2023.